Ecosystems
https://doi.org/10.1007/s10021-021-00628-6

Coupled Shifts in Ectomycorrhizal Communities and Plant Uptake of Organic Nitrogen Along a Soil Gradient: An Isotopic Perspective

Peter T. Pellitier,[1,3]* Donald R. Zak,[1,2] William A. Argiroff,[1] and Rima A. Upchurch[1]

[1]*School for Environment and Sustainability, University of Michigan, Ann Arbor, Michigan 48109, United States of America;*
[2]*Department of Ecology and Evolutionary Biology, University of Michigan, Ann Arbor, Michigan 48109, United States of America;*
[3]*Department of Biology, Stanford University, Stanford, California 94305, United States of America*

Abstract

Plants associating with mutualistic ectomycorrhizal (ECM) fungi may directly obtain nitrogen (N) bound in soil organic matter (N-SOM). However, the contribution of N-SOM to plant growth under field conditions remains poorly constrained. We tested the hypothesis that turnover in ECM communities along soil inorganic N gradients mediates a functional transition from plant reliance on N-SOM in low inorganic N soils, to primarily inorganic N uptake in inorganic N-rich condition soils. We quantified the δ^{15}N of *Q. rubra* foliage and roots, organic and inorganic soil N pools, and used molecular sequencing to characterize ECM communities, morpho-traits associated with N-foraging, and a community aggregated sporocarp δ^{15}N. In support of our hypothesis, we document the progressive enrichment of root and foliar δ^{15}N with increasing soil inorganic N supply; green leaves ranged from − 5.95 to 0.16‰ as the supply of inorganic N increased. ECM communities inhabiting low inorganic N soils were dominated by the genus *Cortinarius*, and other fungi forming hyphal morphologies putatively involved in N-SOM acquisition; sporocarp estimates from these communities were enriched (+ 4‰), further supporting fungal N-SOM acquisition. In contrast, trees occurring in high inorganic N soils hosted distinct communities with morpho-traits associated with inorganic N acquisition and depleted sporocarps (+ 0.5‰). Together, our results are consistent with apparent tradeoffs in the foraging cost and contribution of N-SOM to plant growth and demonstrate linkages between ECM community composition, fungal N-foraging potential and foliar δ^{15}N. The functional characteristics of ECM communities represent a mechanistic basis for flexibility in plant nutrient foraging strategies. We conclude that the contribution of N-SOM to plant growth is likely contingent on ECM community composition and local soil nutrient availability.

Key words: Plant–soil interactions; Soil organic matter; Organic nitrogen; Isotopes; Ectomycorrhizal fungi; Plant growth; Ecosystem ecology.

Received 8 September 2020; accepted 27 February 2021

Supplementary Information: The online version contains supplementary material available at https://doi.org/10.1007/s10021-021-00628-6.

Author Contributions PP, DZ, and WA conceived of the study. All authors contributed to data collection. PP analyzed data with input from DZ and WA. PP wrote the paper and all authors provided constructive edits.

**Corresponding author; e-mail:* ptpell@stanford.edu

Published online: 26 April 2021

Highlights

- Symbiotic mycorrhiza allow plants to obtain locally abundant forms of limiting nutrients
- Nitrogen isotopes reveal the contribution of soil N sources to plant growth
- Organic nitrogen does not ubiquitously contribute to the growth of host trees

Introduction

Elucidating the microbial interactions controlling the availability of limiting plant nutrients remains a key research priority that holds promise to inform global models of plant response to climate change (Näsholm and others 2009; Wieder and others 2015). The majority of plants associate with mycorrhizal root symbionts to alleviate nutrient limitation (Smith and Read 2010; Genre and others 2020). Arbuscular (AM) and ectomycorrhizal (ECM) fungi represent two of the main types of mycorrhiza, and the mycorrhizal-associated nutrient economy (MANE) framework has identified fundamental differences in the role of AM and ECM fungi in ecosystem processes (Phillips and other 2013; Averill and others 2019). One cornerstone of this framework is that ECM fungi forage for nitrogen (N) organically bound in soil organic matter (N-SOM) and transfer this source of N to their plant host, whereas AM plant hosts are reliant upon inorganic N alone (Read 1991; Phillips and others 2013).

An unresolved question is the extent to which ECM communities differ in their capacity to access N-SOM and transfer this N to their plant source (Zak and others 2019). Understanding this variation is essential, because distinct ECM communities are often conceptualized to function similarly in their capacity to provision N-SOM to their plant host. The possibility that association with ECM fungi allows plants to 'short-circuit' supply rates of inorganic N (that is, net N mineralization) has significant implications for predicting plant productivity responses to elevated atmospheric CO_2 (Terrer and others 2016, 2019), modifying the outcomes of plant competition (Corrales and others 2016) and soil C dynamics (Orwin and others 2011; Zak and others 2019). However, ECM fungi have repeatedly evolved, approximately 85 times (Tedersoo and Smith 2013), from a wide ecological array of fungal ancestors, and their genomic potential to decay SOM varies widely among ECM lineages (Kohler and others 2015; Pellitier and Zak 2018; Miyauchi and others 2020). The evolution of the ECM lifestyle has generally resulted in massive loss of genes involved in SOM decay (Kohler and others 2015; Miyauchi and others 2020). However, these gene losses have not been equal across ECM lineages (Pellitier and Zak 2018). Although certain ECM has highly reduced genomic potential to produce hydrolytic and oxidative enzymes mediating SOM decay (Wolfe and others 2012), others such as the genus *Cortinarius* or *Piloderma* have gene repertoires that rival certain freeliving white-rot saprotrophs (Bödeker and others 2009). Understanding factors structuring the geographic distribution of distinct ECM lineages is critical for building synthetic understanding of the contribution of N-SOM to plant growth.

Studies at local, regional, and continental scales consistently identify soil inorganic nitrogen (N) availability as a key factor structuring ECM communities (Taylor and others 2000; Lilleskov and others 2002; Peay and others 2015; van der Linde and others 2018). Soil inorganic N availability may also impact the functional attributes of ECM communities (Lilleskov and others 2002; Courty and others 2016), which could feedback to influence plant nutrition. For example, plants inhabiting low inorganic N availability soils host ECM taxa with morphological characteristics (Moeller and others 2014; Defrenne and others 2019), enzyme profiles (Tedersoo and others 2012; Courty and others 2016; Sterkenburg and others 2018), and isotopic signatures (Hobbie and Agerer 2010; Kranabetter and MacKenzie 2010) consistent with enhanced SOM decay potential. Linking these fungal characteristics with plant uptake of N-SOM has proven challenging; however, there remains minimal evidence for the generalized, greater relative contribution of N-SOM to plant growth in low inorganic N availability soils, particularly in temperate forest ecosystems (Zak and others 2019). Because the decay of SOM is thought to be metabolically costly (Lindahl and Tunlid 2015), these patterns are broadly congruent with understanding of biological market perspectives whereby plants associate with fungi that optimize resource acquisition while minimizing C cost (Christian and Bever 2018). Indeed, organic N in the form of amino acids and proteins may primarily contribute to plant N budgets under conditions of low inorganic N availability (Kielland 1994; Nordin and others 2004; Jones and others 2005; Näsholm and others 2009). The contribution of N-SOM to plant growth may also follow similar patterns (Read and Perez-Moreno 2003; Koide and others 2014).

Comparison of δ^{15}N among plant tissues, fungal sporocarps, and soils offers insights into plant assimilation of distinct N sources, including N-SOM (Michelsen and others 1996; Robinson 2001; Hobbie and Hobbie 2006). For example, foliage of ericoid mycorrhiza and ECM plants is generally depleted in δ^{15}N, relative to AM-associated and N fixing plants (Craine and others 2009), which is considered broadly indicative of their capacity to provision the plant host with N derived from organic sources (Michelsen and others 1996, 1998; Craine and others 2009; Mayor and others 2015; Averill and others 2019). There remains considerable variation among ECM-associated foliar δ^{15}N that remains poorly explained (Hobbie and Högberg 2012). In particular, foliar δ^{15}N for ECM-plants exhibits large shifts across soil inorganic N gradients; foliage becoming relatively enriched as inorganic soil N availability increases (Hobbie and others 2000; Pardo and others 2006; Kranabetter and MacKenzie 2010).

There are two main hypothesized mechanisms whereby ECM communities can modify foliar δ^{15}N. First, because ECM hyphae fractionate N transfer products, delivering relatively more depleted ^{14}N to the host, while retaining a greater proportion of ^{15}N in their hyphae and sporocarps (Hogberg and others 1999; Kohzu and others 2000; Hobbie and Colpaert 2003), a larger proportion of N passing through ECM hyphae results in comparatively depleted plant tissue (Michelsen and others 1996; Hobbie and Agerer 2010; Mayor and others 2015). Secondly, the biochemistry of soil N that ECM fungi assimilate may impact both relative intra-hyphal fractionation as well as the δ^{15}N that plants receive. The δ^{15}N of organic and inorganic soil N pools can vary significantly, and δ^{15}N-SOM may be enriched relative to dissolved organic nitrogen (DON) and inorganic N sources (Melillo and others 1989; Yano and others 2010; Hobbie and Högberg 2012). All things equal, plants reliant on N-SOM sources may have relatively depleted tissues due to greater relative intra-hyphal fractionation (Werner and Schmidt 2002; Yano and others 2010) while ECM fungi would have enriched hyphae and sporocarps (Michelsen and others 1996; Hobbie and Hobbie 2006; Hobbie and Agerer 2010). In contrast, if ECM communities primarily provision their hosts with inorganic N, plants and ECM sporocarps may both have δ^{15}N that more closely reflects the δ^{15}N of soil inorganic N (Hobbie and Hobbie 2006, 2008). This logic is conceptually akin to mechanisms proposed to explain patterns of δ^{15}N observed among ERI, ECM and AM plant foliage (Craine and others 2009; Averill and others 2019). While these two mechanisms are not mutually exclusive, they are rarely studied in relation to plant δ^{15}N dynamics (Michelsen and others 1998; Lilleskov and others 2002; Hobbie and Hobbie 2006).

We studied plant and soil δ^{15}N, and ECM communities along a natural soil inorganic N gradient to evaluate shifts in the contribution of N-SOM to *Quercus rubra* L individuals. We characterized ECM communities using molecular sequencing, estimated community aggregated ECM sporocarp δ^{15}N values using global databases and quantified the relative abundance of ECM root-tips on individual root-systems. Foremost, we predicted that ECM communities occurring in low inorganic N soils have a greater abundance of ECM root-tips and greater capacity to forage for N-SOM. Together these factors should result in *Q. rubra* tissues being relatively depleted (smaller δ^{15}N). In contrast, trees occurring in high inorganic N soils may associate with ECM communities that predominately forage for inorganic N, and be less reliant overall upon ECM for N uptake. Under these conditions, we predict that tree tissue will be comparatively enriched. Finally, we predict that community aggregated estimates of ECM sporocarp δ^{15}N values will be inversely related with soil inorganic N availability if ECM communities exhibit functional shifts across the soil gradient.

Methods

Sampling Sites

Sixty mature *Quercus rubra* L. individuals were sampled across a natural soil inorganic nitrogen gradient in Manistee National Forest in northwestern Lower Michigan (Supplementary Figure S1). All 60 trees studied here are approximately 100 years old, resulting from regrowth following forest clearing in the early twentieth century. This soil gradient has been extensively characterized, and relative differences among soils studied here have persisted for decades (Zak and others 1986; Zak and Pregitzer 1990; Edwards and Zak 2010). Annual rates of net N mineralization, an estimate of inorganic N availability, range from 38 to 120 kg N ha^{-1} y^{-1} (calculated from Zak and Pregitzer 1990), which broadly spans soil inorganic N availability in the upper Lake States region (Pastor and others 1984; McClaugherty and others 1985). Variation in nutrient cycling in this region is derived from micro-site climatic differences in nutrient and water retention that have developed in the past approximately 10,000 years (Zak and others

1986). An interlobate moraine transects the study region, and a network of outwash plains with slightly coarser textured soils are associated with lower rates of net N mineralization; in contrast, soils occurring in more upland positions on moraines are associated with greater rates of net N mineralization. The 60 individual trees inhabited 12 forest stands, which are broadly representative of ecosystem classifications previously developed for this region (Zak and others 1986; Zak and Pregitzer 1990). Soils across the study region are derived from sandy (~ 85% sand) glacial drift, and range from Typic Udipsamments to Entic Haplorthods. Because the sampling region is relatively small, with the most distant sites being about 50 km apart (Figure S1), all trees experience the same macro-climatic conditions. Each stand was approximately 1 ha in size. Within each stand, five mature *Q. rubra* individuals that were at least 10 m apart were randomly selected (using a random number generator) and sampled. All trees occur within an elevation band of 70–130 m (Zak and others 1986). The length of the growing season is approximately 100–120 days, and mean annual temperature is approximately 7.3 °C.

Soil, Leaf and Root Sampling

In May 2018, 5 root cores were collected radially around the dripline of each focal *Q. rubra* individual in order to harvest fine roots; cores were 10-cm deep and 121 cm^2 (11 × 11 cm square). Five additional soil cores (5 cm diameter, 10 cm deep after removing litter layer) were collected immediately adjacent (within 20 cm) to the root cores for subsequent analysis of edaphic characteristics. Soil and root cores were stored on ice and immediately transported to the laboratory. Soil was also collected in an identical manner around the same focal trees in August 2018 for additional edaphic characterization. Full-sun green leaves were collected from the top of the forest canopy for each focal tree in August 2019 using a 20-gauge shotgun. *Q. rubra* leaves were identified and collected from the uppermost forest floor (Oi horizon) in early May 2019 within 3.5 m of the base of each focal tree, representing senesced leaves from the 2018 growing season.

Senesced leaves and green leaves (~ 7 leaves each) were prepared for stable isotope analysis by deveining, homogenizing and drying at 60 °C for 48 h. Leaves were then ground using a ball mill. Leaves with necrotic regions or visible discoloration (< 5%) were not included. Bulk soil was also prepared for stable isotope analysis by homogenizing the aforementioned soil cores at the individual tree-level, passing the material through a 2-mm sieve, drying at 105 °C for 12 h, and grinding with a ball mill (n = 60). Root cores were homogenized on a site-level basis, fine roots (< 0.5 mm diameter), and first through third-order roots were selected rinsed of adhering soil particles and dried at 60 °C for 48 h. The majority of co-occurring roots present were *Acer rubrum*, which is easily distinguished from *Q. rubra, A. rubrum* roots were removed from the pooled samples. Three 1-g subsamples of the stand-level root composite were then dried and ground for isotope analysis as described above (n = 36).

Freshly sieved soil extracts (May sampling: 1:2 soil: 2 M KCl) were used to determine the $\delta^{15}N$ of extractable inorganic and organic N (dissolved organic nitrogen; DON). NH_4^+ and NO_3^- were sequentially diffused onto individual acid traps for seven days each using MgO followed by Devarda's metal (Brooks and others 1989). To measure $\delta^{15}N$-DON we used a persulfate digest on soil extracts to convert DON to NO_3^- and diffuse onto new acid traps (Cabrera and Beare 1993). Acid traps were then encapsulated for stable isotope analysis. $\delta^{15}N$ for each plant tissue and soil component was measured using a PDZ Europa ANCA-GSL elemental analyzer interfaced to a PDZ Europa 20–20 isotope ratio mass spectrometer (Sercon Ltd., Cheshire, UK), at the University of California Davis, Stable Isotope Facility. Stable isotope abundances are reported as $\delta^{15}N$ in parts per mil (‰). Samples with more of the heavy isotope are referred to as enriched; samples with less of the of heavy isotope are referred to as depleted (Robinson 2001).

Soil mineralization rates and total free primary amines (TFPA) in soil solution were quantified for soil samples collected in both May and August 2018. Soil inorganic N was extracted from fresh sieved soil using 2 M KCl, followed by a 14-day aerobic incubation assay in order to measure rates of soil inorganic N mineralization (Vitousek 1982). NO_3^- and NH_4^+ in soil extracts were analyzed colorometrically (AQ2; Seal Analytical, Mequon, WI). Aerobic incubations of inorganic N were conducted following Vitousek (1982). TFPA in soil (primarily amino acids and amino sugars) was measured using fresh sieved soil extracted with 2 M KCl following Darrouzet-Nardi and others (2013). These extracts were identical to those used to measure extractable NO_3^- and NH_4^+ prior to aerobic incubation. TFPA is expressed as µmol leucine equivalents, because leucine was used as the analytical standard; estimates of TFPA availability may be considered relative indices of labile organic N

availability in soil solution (Darrouzet-Nardi and others 2013). Total C and N contents of bulk soil (% of dry mass) were determined using combustion analysis on a LECO TruMac CN analyzer (LECO Corporation, St. Joseph, MI, USA) for soil collected in May 2018. Soil pH was determined for 2:1 deionized water-soil slurries with an Accumet 15 pH meter for soil collected in August 2018 (Fisher Scientific, Waltham, MA, USA).

Understory Plant Community Sampling

In May 2020, we located focal *Q. rubra* trees, and estimated the percent cover of all understory plant stems, present in $1m^2$ square sampling quadrats in two replicate quadrats. Quadrats were placed at random azimuths from the base of the focal tree at a distance of 3 m. Percent cover was averaged between the replicate plots at the individual tree basis.

Ectomycorrhizal Community Characterization

In August of 2018, ectomycorrhizal root-tips were isolated from five individual ''ECM cores'' taken immediately adjacent (at most 25 cm) to the aforementioned soil and root cores. Surface litter was removed, and ECM cores were 10 cm deep and $121cm^2$ (11×11 cm square). ECM cores were pooled for each individual focal tree and ECM tips were manually excised using a dissecting microscope after visually eliminating all non-*Quercus* roots. Definitive ectomycorrhizal tips on *Quercus rubra* were collected after visual confirmation of ECM mantle and high turgor (Agerer 2001). Root-tip sampling was standardized across samples by visually assessing the tips of at least 90% (wet weight) of all *Quercus* roots collected for individual focal trees. Samples were stored at 4 °C and processed within 12 days of field sampling.

In total, 14,944 individual ECM root-tips were excised, rinsed in 2% cetyl trimethyl ammonium bromide (CTAB) supplemented with 0.8% ß-mercaptoethanol, and then frozen in fresh 2% CTAB at − 80 °C. CTAB was removed after thawing samples, and root-tips were lyophilized for 12 h. Tips were then weighed using a microbalance and DNA was extracted from the totality of each sample, using two or three individual DNA extraction columns; each extraction utilized about 10 mg of lyophilized root-tip per extraction, so as not to bias extraction efficiencies. The ITS2 fragment of rRNA was amplified using PCR, following Taylor and others (2016). PCR libraries were barcoded using dual indexed Illumina primers, cleaned using AMPure XP, and sequenced using Illumina Mi-Seq (2×250; San Diego, CA) at the University of Michigan Microbial Systems Molecular Biology Laboratory.

Illumina sequencing generated a total of 27,274,716 raw reads that were demultiplexed, and forward reads were processed using DADA2 and clustered into absolute sequence variants (ASV) and assigned taxonomy using the UNITE dynamic database (v.8) (Nilsson and others 2019). Communities were analyzed after rarefying samples to 24,021 sequences. ASV were collapsed to species level assignment and taxa that could not be assigned to Kingdom Fungi, and appeared less than twice across all samples were removed. The ectomycorrhizal status of fungal genera was assigned using literature searches (Tedersoo and Smith 2013), and fungal taxa with uncertain or non-ECM status were removed from subsequent analyses ($\sim$ 20% of overall sequences). We used the DEEMY (characterization and DEtermination of EctoMYcorrhizae) database (http://www.deemy.de/) to gather morphological information on the exploration type (hyphal foraging distance) and rhizomorph occurrences of ECM taxa present in our dataset at more than 0.05% relative abundance. We assigned morphological data for 28 ECM genera comprising more than 93% of all identified ECM sequences. The full root-tip sampling and molecular sequence processing protocol is described in full (Supplementary Methods).

Community-Wide Estimates of ECM $\delta^{15}N$

Sporocarp surveys present significant challenges to the estimation of the $\delta^{15}N$ of composite ECM communities (Kranabetter and MacKenzie 2010). Foremost, surveys are labor-intensive due to the sporadic and asynchronous nature of fungal fruiting, resultant analyses generally suffer from low community coverage. Many ECM fungi also do not fruit annually, and some do not produce conspicuous fruiting bodies, resulting in missing representation for certain lineages. Additionally, sporocarp diversity and biomass rarely reflect the occurrence of fungi forming ECM root-tips (Gardes and Bruns 1996). Finally, ECM sporocarps sampled near an individual tree can rarely be linked with specific root-systems (Smith and others 2011), obfuscating the relationship between foliar $\delta^{15}N$ and sporocarp $\delta^{15}N$.

To minimize many of these limitations, we used an alternative procedure to estimate community-weighted $\delta^{15}N$ sporocarp values for ECM commu-

nities inhabiting individual *Q. rubra* root-systems. We employed a global database of ^{15}N values for ECM fungal sporocarps compiled by Mayor and others (2009), in conjunction with the relative ITS2 sequence abundance of each genus detected on each root-system. The relative sequence abundance of each genus was multiplied by their sporocarp $\delta^{15}N$ estimate, and the components were then summed for all genera present on individual trees (samples), producing an community weighted sporocarp $\delta^{15}N$ estimate. The global database contained a total of 961 sporocarp observations spanning 21 genera (Mayor and others 2009). Two observations of *Hebeloma* sporocarps in the global dataset were extremely enriched (+ 20‰) and were removed from our analysis. Similar to Mayor and others (2009), we calculated mean $\delta^{15}N$ values for each genus (Supplementary Table 1). Because not all ECM genera we detected in our field plots were represented by published $\delta^{15}N$ sporocarp observations, we also calculated the relative abundance of ECM sequences, on a per-tree basis, for which $\delta^{15}N$ sporocarp values could be ascribed.

Statistical Analysis

Rates of net N mineralization were calculated by summing the concentrations of NO_3^- and NH_4^+ prior to and following aerobic incubation; net N mineralization was the difference between these values, and mineralization rates are expressed on a dry soil basis. To examine relationships among soil $\delta^{15}N$, sporocarp $\delta^{15}N$ and plant $\delta^{15}N$, we used best-fit regression functions (generally linear) and correlation analysis (Pearson-product moment). In addition, to account for potential non-independence among trees (samples) as a result of spatial proximity within stands, we accounted for the exact distance among trees using distances calculated from GPS coordinates. To achieve this, we used linear mixed effect (LME) models to individually assess the relationship between soil mineralization rates, and leaf $\delta^{15}N$ (green and senesced), and sporocarp estimates, taking into account the underlying spatial sampling structure, using a gaussian correlation structure. Euclidean distances among trees were calculated and restricted maximum likelihood estimation was conducted using the package nlme 3.1 (Pinheiro and others 2020). Residuals were plotted to check for violations of normality. Due to the stand-level sampling conducted for the root samples, statistical models were not conducted for root samples.

We used multivariate generalized linear models (GLM) to test the effect of soil chemistry on the composition of ECM communities, using the R. package *mvabund* version 4.0.1; this analysis was achieved using Hellinger transformed counts, and a negative binomial distribution (Wang and others 2012). Abiotic parameters (pH, soil N, C:N, August net N mineralization) were also included in the model without interaction terms and model residuals were visually assessed. The effect of predictor variables was quantified using likelihood-ratio tests (ANOVA, pit trap resampling, 1000 bootstraps) with Bonferonni correction using the 'summary.manyglm' command. To study the effect of ECM community composition on green leaf $\delta^{15}N$, we used a partial Mantel test in the Vegan package v. 2.5.6 to compare distance matrices based and Hellinger-transformed abundances of ECM taxa. Geographic distances among individual trees were calculated using the R package Geosphere 1.5–10, prior to incorporation in the model. All analyses were conducted using R 4.0.2.

Results

We re-established the underlying soil inorganic N gradient in this region. We confirmed that variation in soil inorganic N availability across stands was consistent across the growing season; soil samples obtained from under the same canopies in May and August 2018 were highly correlated (Pearson r = 0.77; Figure S2). The mean stand level coefficient of variation was 38% for August soil sampling, which provided a continuous range of net N mineralization values across a range of scales, and hence inorganic N supply (Figure S3). Green-leaf δ^5N increased across the soil inorganic N gradient, ranging from highly depleted -5.95‰ in low inorganic N sites to + 0.16‰ where inorganic N availability was high (linear fit: $P < 0.001$, $R^2_{adj} = 0.60$; third-order polynomial fit $P < 0.001$, $R^2_{adj} = 0.63$; LME (spatially explicit model): $t = 9.185$, $P < 0.0001$), as did the relationship for senesced leaves (range = − 5.55‰ to + 0.91‰, linear fit: $P < 0.001$, $R^2_{adj} = 0.57$, third-order polynomial fit $P < 0.001$, $R^2_{adj} = 0.59$; LME: $t = 8.56$, $P < 0.0001$, Figure 1). Green-leaf N concentrations ($R^2_{adj} = 0.36$, $P < 0.001$; LME: $t = 5.23$, $P < 0.001$) and senesced leaf N concentrations ($R^2_{adj} = 0.35$, $P < 0.001$; LME: $t = 5.42$, $P < 0.001$) were both positively correlated with inorganic N availability (Figure S4-5). Analytical variance for green leaf samples run in duplicate ranged from 0.00 to 0.16‰. Similar to foliage, root $\delta^{15}N$ became progressively enriched across the gradient (Figure 1).

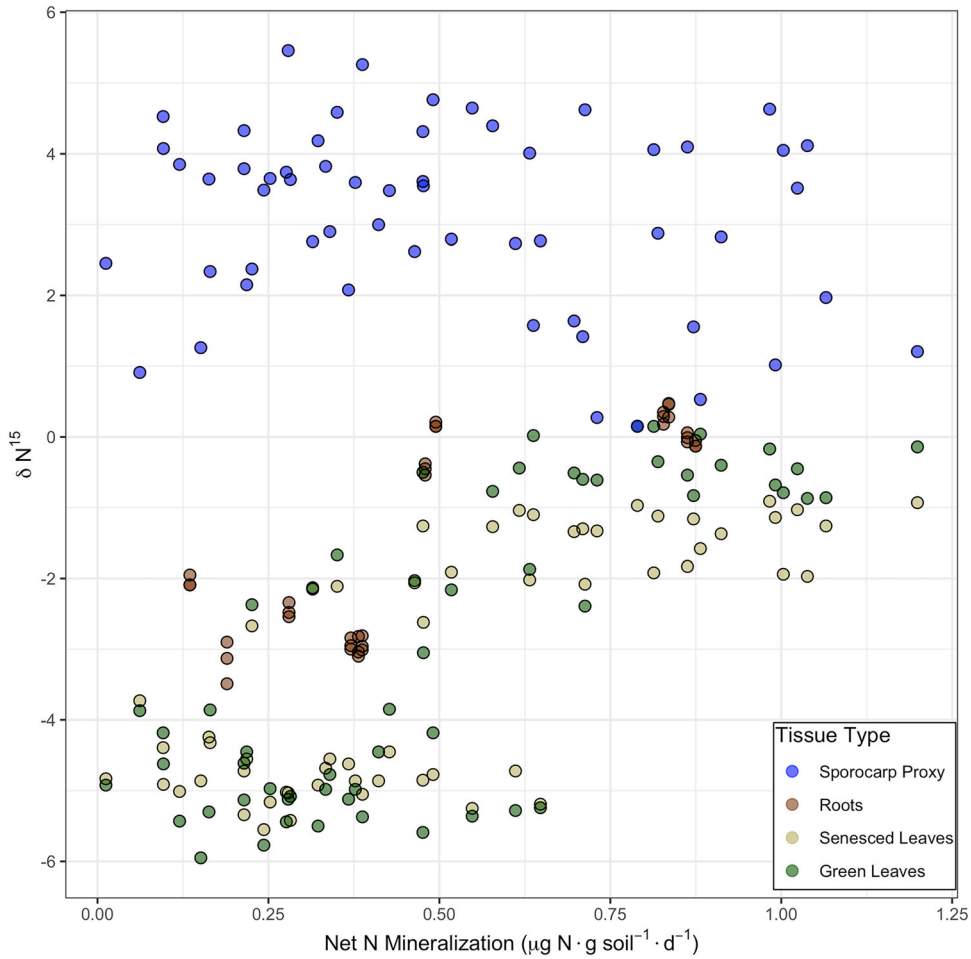

Figure 1. $\delta^{15}N$ of plant components: green-leaf foliage, senesced leaves, and roots along the gradient of net N mineralization rates (x-axis). Blue points represent community weighted mean proxies for the $\delta^{15}N$ of ECM sporocarps. Mineralization rates are presented for soil sampled in August 2018. Root-samples represent replicates at the site level (n = 12), and are plotted as site-level means

The proportion of NO_3^- present in soil solution (unincubated soils) increased across the gradient (Figure S6-7) for both May and August sampling time points. $\delta^{15}N$–NO_3^- became significantly depleted (linear fit: $R^2_{adj} = 0.09$, $P < 0.05$), whereas $\delta^{15}N$–NH_4^+ became progressively enriched in higher inorganic N soils (linear fit: $R^2_{adj} = 0.29$, $P < 0.001$; Figure S8). When the $\delta^{15}N$ of inorganic N available in soil solution was weighted by the proportional abundance of NO_3^- and NH_4^+ present in each unincubated sample, the $\delta^{15}N$ of the weighted inorganic N pool did not significantly vary across the gradient (LME; $t = -1.70$, $P = 0.094$; Figure 2). Rates of nitrification, calculated as the difference in the abundance of NO_3^- between incubated and unincubated soils (Zak and Grigal 1991) generally increased with rates of net N availability, whereas ammonification decreased (Figure S9-10). In contrast, SOM $\delta^{15}N$ increased significantly across the gradient (linear fit: $R^2_{adj} = 0.39$, $P < 0.001$; LME; $t = 5.90$, $P < 0.0001$; Figure 2). Finally, the $\delta^{15}N$ of dissolved organic nitrogen (DON) did not vary across the soil N gradient (linear fit: $P = 0.22$; Figure 2; LME: $t = 1.39$, $P = 0.17$), and the measured pool of total free primary amines (TFPA) in soil solution did not vary across the soil inorganic N gradient (Figure S11).

Sequencing depth adequately captured fungal diversity present in each sample (Figure S12), and the proportion of sequences ascribed ECM status did not significantly vary across samples (Figure S13). Non-ECM taxa are presented in Supplementary Table 14. Inorganic N availability was a strong predictor of shifts in ECM community composition (GLM: $Wald_{adj}$: 4.86, $P < 0.001$), and C:N ($Wald_{adj}$: 5.10, $P < 0.001$) and pH ($Wald_{adj}$: 4.41, $P < 0.001$) also emerged as significant predictors. Notably, the abundance of ECM genera

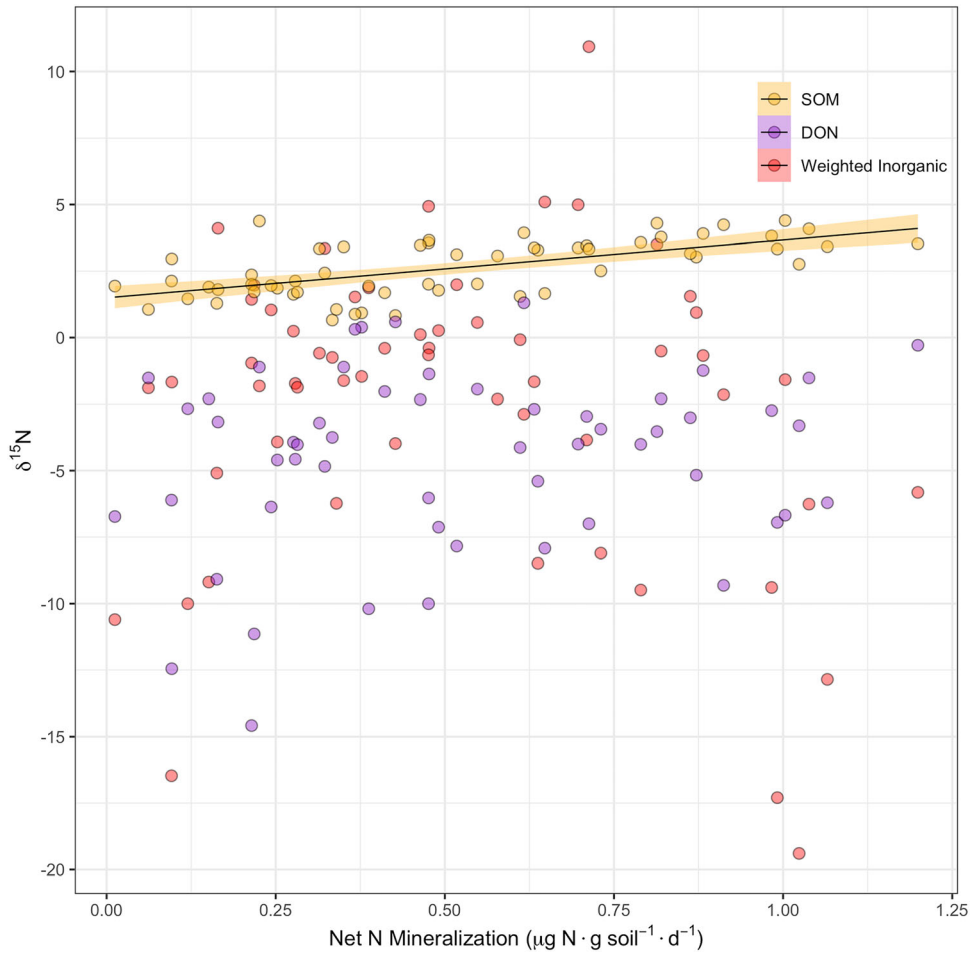

Figure 2. Relationship between soil N sources and their δ^{15}N across the soil N gradient. The δ^{15}N of N-SOM increased significantly: $R^2_{adj} = 0.39$, $P < 0.001$ (linear fit), whereas no significant differences in δ^{15}N DON or the standing inorganic N pool were observed. The inorganic N pool is weighted by the relative abundance of ammonium and nitrate present in unincubated soils, multiplied by the δ^{15}N of each compound class for each sample. Mineralization rates are presented for soil sampled in August 2018

such as *Cortinarius* and *Hebeloma* were inversely correlated with soil inorganic N (Figure 3). In contrast, *Russula* and *Tomentalla* were positively associated with increasing soil inorganic N availability which is consistent with their ''nitrophilic'' niche requirements (Suz and others 2014; van der Linde and others 2018).

Compositional turnover in ECM communities was associated with shifts in the presence of hyphal morphologies involved in N-foraging (Figure 4). The relative sequence abundance of medium-distance exploration types (linear fit: $R^2_{adj} = 0.46$, $P < 0.0001$: LME: $t = -6.6$, $P < 0.0001$ (two outliers removed), and fungi forming rhizomorphic hyphae (linear fit: $R^2_{adj} = 0.28$, $P < 0.0001$; LME: $t = -3.81$, $P = 0.0003$) were negatively correlated with foliar δ^{15}N (Figure 4). The proportion of ECM sequences assigned morphological attributes using DEEMY also did not vary across samples ($P = 0.50$). The abundance and biomass of ECM root-tips declined significantly across the inorganic N gradient (root-tip count: linear fit: $R^2_{adj} = 0.25$, $P < 0.001$; LME: $t = -4.21$, $P < 0.001$; root-tip weight: linear fit: $R^2_{adj} = 0.10$, $P < 0.01$; LME: $t = -2.71$, $P = 0.009$) (Figure S15-16). Green-leaf δ^{15}N was inversely related to the number (linear fit: $R^2_{adj} = 0.31$, $P < 0.001$; LME: $t = -2.80$, $P = 0.0070$) and weight of ECM root-tips (linear fit: $R^2_{adj} = 0.18$, $P < 0.001$; LME: $t = -3.71$, $P < 0.0001$). Finally, there was a significant positive correlation in ECM community dissimilarity and green leaf δ^{15}N (partial Mantel r = 0.06, $P = 0.04$).

The global database of sporocarp δ^{15}N measurements allowed us to assign values to ECM genera representing an average of 69% of all sequences detected in each sample. Critically, the proportion

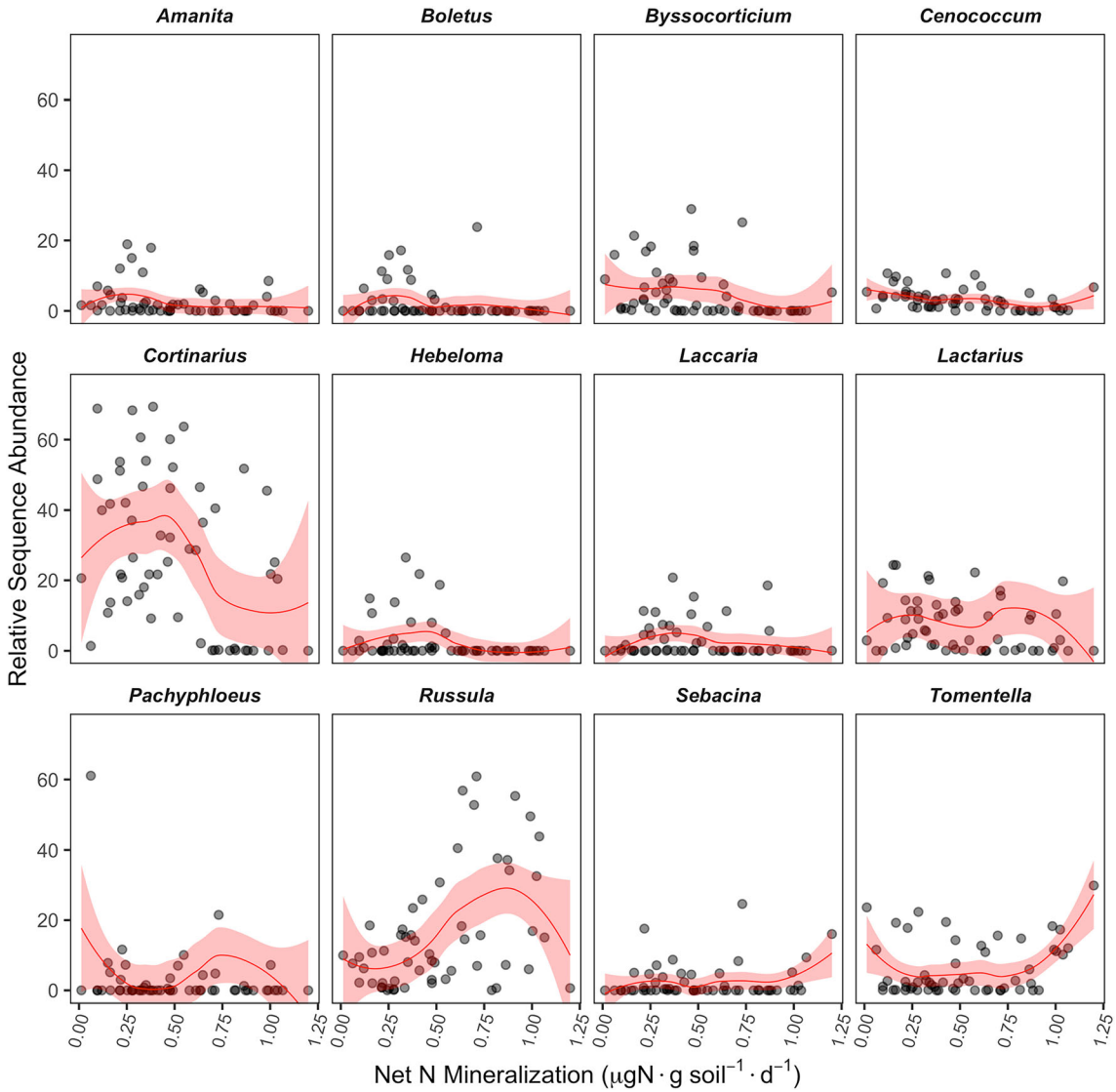

Figure 3. Relative abundance of dominant ECM genera (headings) representing more than 2% of sequences across all samples. Red lines represent smoothed loess splines. X-axis indicates net N mineralization rates which estimate soil inorganic N availability. Mineralization rates are presented for soil sampled in August 2018

of sequences annotated with ECM sporocarp δ^{15}N values did not vary across the inorganic N gradient (linear fit: $P = 0.43$; Figure S17). ECM community weighted δ^{15}N sporocarp estimates were negatively related to inorganic N availability (linear fit: $R^2_{adj} = 0.09$; $P < 0.05$; LME: $t = -1.58$, $P = 0.12$, Figure 1). When we subset the foliar database to exclusively use sporocarp accessions derived from sampling locations between 5 and 10 °C; we again detected an inverse linear relationship between soil mineralization rates and sporocarp δ^{15}N (linear fit: $P = 0.03$). All accessions are retained in the presentation of Figure 1 and associated analyses. Standard errors for individual genera are reported in Supplementary Table 1. Multiplying δ^{15}N sporocarp estimates by the number of ECM root-tips present on individual root-systems, thereby taking into account estimates of shifts in the number of ECM root-tips along the gradient, strengthens the negative relationship between sporocarp δ^{15}N estimates and inorganic N availability (linear fit: $R^2_{adj} = 0.19$, $P < 0.001$; LME: $t = -3.68$, $P < 0.0001$). Finally, on a per-tree-basis, there was a significant and negative relationship between sporocarp δ^{15}N estimates, and green-leaf δ^{15}N (linear fit: $R^2 = 0.11$, $P < 0.01$; LME: $t = -3.07$, $P = 0.003$), that was also supported when sporocarp values were scaled by the number of colonized ECM root-tip (linear fit $R^2_{adj} = 0.30$; LME: $t = -3.16$, $P = 0.003$). For four

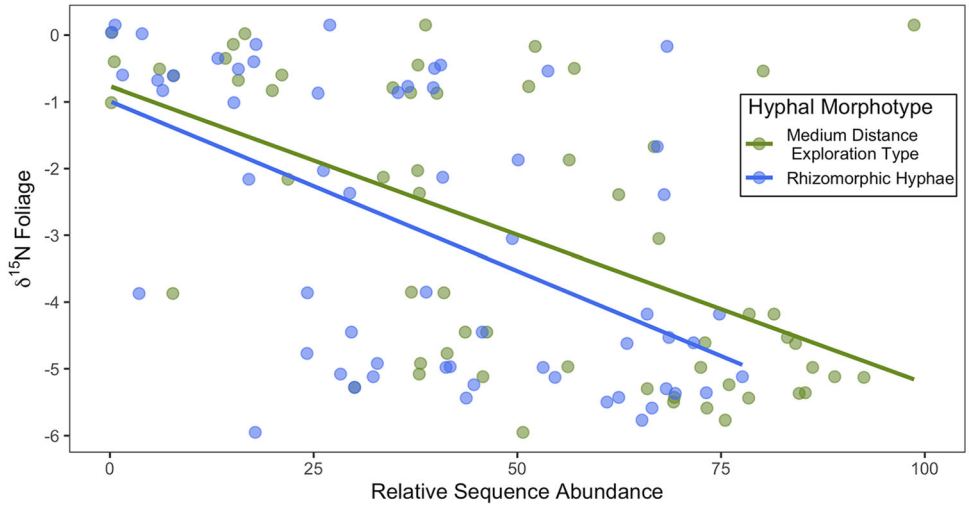

Figure 4. Relative sequence abundance of rhizomorphic and medium-distance exploration types and green-leaf δ^{15}N. ECM communities were characterized from the same focal *Q. rubra* trees from which leaves were sampled. Roots and senesced leaves follow similar patterns. Lines indicate linear fits, $P < 0.001$ for both panels. The spatially explicit LME model was also highly significant when two significant outliers, with very high proportions of medium distance exploration types were removed. Individual ECM taxa can form both medium distance exploration types and rhizomorphic hyphae

samples, less than 25% of all sequences could be attributed to ECM genera with known δ^{15}N sporocarp values (Figure S17); removing these samples did not change the trends or overall significance of the relationship between foliar δ^{15}N and sporocarp δ^{15}N (linear fit: $P = 0.04$; LME: $P = 0.007$), but the relationship between mineralization rates and sporocarp δ^{15}N values was rendered insignificant (linear fit: $P = 0.09$). No understory N-fixing taxa were detected that could contribute to unmeasured inorganic N availability (Figure S18).

Discussion

To evaluate the hypothesis that N-SOM primarily contributes to plant growth under conditions of low inorganic N supply, we studied the δ^{15}N of *Q. rubra* leaves and roots, inorganic and organic soil N pools and ECM fungal communities along a natural soil inorganic N gradient. Our results suggest that turnover in the N foraging potential of ECM communities mediates a transition from plant reliance on N-SOM in low inorganic N soils, to inorganic N in soils in which inorganic N is plentiful. This work provides some of the strongest evidence to date that N-SOM can contribute to temperate tree N budgets. Specifically, foliar δ^{15}N for trees occurring in inorganic N-rich soils were equally, if not more enriched than global mean values for AM-associated plants, which are entirely dependent on inorganic N (Craine and others 2009). In contrast, *Q. rubra* foliage occurring in low inorganic N sites, matched mean global values for ericaceous (ERI) plants, thought to be heavily dependent on organic N sources (Craine and others 2009). Together, this work extends existing mycorrhizal nutrient economic frameworks by documenting that plant access to N-SOM may be dependent upon ECM community composition and decay trait-tradeoffs that favor ECM N-SOM decay capacity in low inorganic N soil conditions.

ECM fungi act as an important intermediary between soil and plant δ^{15}N, and this study offers insight into how fungal N-foraging may generate wide intraspecific variation in foliar δ^{15}N. Taxonomically, ECM communities inhabiting soils with low inorganic N availability were dominated by the genus *Cortinarius,* which has been extensively implicated in the acquisition of N-SOM (Bödeker and others 2014; Kohler and others 2015; Sterkenburg and others 2018). In contrast, soils with high inorganic N availability were dominated by *Russula* and *Tomentella*; many representatives from these genera have limited genomic capacity to obtain N-SOM (Avis 2012; Sterkenburg and others 2018). Additionally, the dominance of hyphal morphologies associated with N-SOM acquisition also declined significantly across the inorganic N gradient, further supporting the idea that compositional changes in ECM communities have functional consequences for plant N uptake (Moeller

and others 2014; Defrenne and others 2019). Notably, foliar $\delta^{15}N$ became progressively depleted as the abundance of specific ECM taxa and morphotypes implicated in the acquisition of N-SOM increases, likely reflecting the contribution of N-SOM to plant N budgets. The patterns of ECM taxonomic and morphological turnover reported here mirror patterns found in a range of ecosystems (Suz and others 2014; Kranabetter and others 2015; van der Linde and others 2018; Defrenne and others 2019), suggesting that greater plant uptake of N-SOM under conditions of low soil N availability may be common.

We used global estimates of ECM sporocarp $\delta^{15}N$ in conjunction with the relative sequence abundance of ECM genera present on individual root-systems to calculate a community-weighted sporocarp $\delta^{15}N$ estimate. While these estimates cannot account for site-level variation (Taylor and others 1997; Kranabetter and MacKenzie 2010) or reflect absolute sporocarp values for the specific forest stands we studied, the narrow intrageneric sporocarp $\delta^{15}N$ variation (CV = $\sim$ 0.77%) strengthens the utility of this approach. Consistent with our predictions, ECM communities occurring in low inorganic N soils were dominated by genera that produce sporocarps that are enriched (+ 4‰), becoming progressively depleted in higher inorganic N soils (+ 0.5‰). The wide divergence between sporocarp and green-leaf $\delta^{15}N$ under conditions of low inorganic N availability, which progressively narrows with increasing rates of net N mineralization, further supports the interpretation of significant assimilation and fractionation of N-SOM where inorganic N availability is low, and limited fungal fractionation of inorganic N under conditions of higher inorganic N availability. Biochemically, fungal assimilation of NH_4^+ and NO_3^- and subsequent conversion to glutamate or glutamine may entail minimal fractionation as compared to fungal assimilation of organic N, followed by deamination, transamination and biosynthesis of amino acids transfer compounds (Werner and Schmidt 2002; Yano and others 2010). Highly depleted sporocarps have previously been associated with 'contact' type hyphal morphologies and efficient inorganic N uptake (Hobbie and Agerer 2010), processes that are consistent with the field-based patterns reported here. These patterns also mirror previous observations of highly enriched ECM sporocarps in N limited boreal forest soils and progressive depletion with increasing N availability (Taylor and others 2003; Kranabetter and MacKenzie 2010; Mayor and others 2015). Due to the limitations of global sporocarp data as applied here, these patterns cannot stand alone but instead provide important context for the functional shifts inferred from taxonomic and morphological study.

Direct plant N uptake may also impact the patterns reported here. For example, the large divergence between plant $\delta^{15}N$ and $\delta^{15}N$-SOM at the low end of the gradient, but the near convergence of foliar $\delta^{15}N$ with the $\delta^{15}N$ of inorganic N in soils with increasing inorganic N availability. These patterns may result from a greater proportion of unfractionated N taken up directly by plants under conditions of high inorganic N availability. Although we did not explicitly calculate percent colonization of ECM root-tips or estimate standing hyphal biomass, we found a reduction in the standardized number of root-tips recovered under conditions of high inorganic N availability. Similar reductions in mycorrhizal colonization are well documented under conditions of high inorganic N availability (Nilsson and others 2005). In contrast, direct plant uptake of N under conditions of low inorganic N availability is unlikely given the high number of ECM root-tips encountered, and the likelihood that ECM percent colonization is very high under these conditions (Taylor and others 1997). Despite the potential for variation in direct plant N uptake across the studied gradient, estimates of the proportion of plant N uptake passing through ECM root-tips commonly exceeds 75% (Hobbie and Högberg 2012). Despite these considerations, because calculation of community-weighted sporocarp $\delta^{15}N$ values is agnostic to the degree of fungal colonization, our results suggest that shifts in ECM community composition may impact plant $\delta^{15}N$ values irrespective of shifts in the proportion of direct plant N uptake.

Consideration of plant and fungal uptake of NH_4^+, particularly under conditions of high inorganic N availability may also prove critical. While relative supply rates of NH_4^+ were reduced in these soils and rates of nitrification appeared high, estimations of nitrification using aerobic laboratory incubations in the absence of plant roots may overestimate NO_3^- production (Zak and others 1990). Supporting this potential, oak-dominated ecosystems occurring on coarse textured soils in the Great Lakes region, similar to those studied here, typically exhibit low net nitrification rates in the field (Pastor and others 1984; Zak and others 1986). When combined with the potential for greater direct plant N uptake under conditions of high inorganic N availability and highly enriched soil $\delta^{15}N$ NH_4^+ values, a transition from plant uptake of NO_3^- to NH_4^+ may moderately contribute to the overall foliar patterns found here.

The contribution of DON to plant growth is also challenging to infer. As measured, standing stocks of DON in soil solution (TFPA), cannot capture rapid fluxes and plant uptake (Inselsbacher and Näsholm 2012). However, the availability of DON was uniformly low across the soil inorganic N gradient, and it was also highly depleted in comparison to foliar and root δ^{15}N. These patterns are consistent with previous studies from this region observing negligible shifts in the availability of soluble peptides across a similar soil fertility gradient (Rothstein 2009). Given that ECM transfer relatively depleted products to the plant host (Hobbie and others 2000), the enriched foliar and root pools (relative to δ^{15}N DON) do not support significant plant assimilation of DON along the studied soil inorganic N gradient.

The isotopic patterns observed for senesced leaves further corroborate the patterns observed for green leaf δ^{15}N suggesting that our inferences are relatively robust across multiple growing seasons. Results from senesced leaves must be carefully interpreted as they are subject to partial decay and leaching during snowmelt, and because they were collected in the vicinity of the focal host tree, their precise origin cannot be determined.

We studied a widespread and ecologically important temperate tree species, gathering essential support for the hypothesis that N-SOM differentially contributes to plant N budgets. Moreover, we primarily attribute the large variation in *Q. rubra* foliar δ^{15}N originates to shifts in the composition and function of associated ECM communities. Projections of gross primary productivity (GPP) under future climatic regimes that posit the widespread contribution of N-SOM to ECM plant growth may need to be readjusted if certain ECM-associated plants have nutrient economies more akin to AM-associated plants (Terrer and others 2016; Averill and others 2019). Although studies in boreal forest ecosystems have long-acknowledged the contribution of organic N sources to plant growth, particularly under conditions of low inorganic N availability (Kielland 1994; Näsholm and others 2009), our work provides some of the strongest evidence to date documenting similar contributions for temperate tree growth. These findings are remarkably consistent with previous research documenting a foliar shift of about 5‰ among boreal plant species occurring across inorganic N gradients (Michelsen and others 1996; Hobbie and others 2000; Kranabetter and MacKenzie 2010). Shifts in the functional attributes of ECM communities may represent a mechanistic basis for flexibility in plant nutrient foraging strategies. Further study of the trait-tradeoffs that impact ECM community assembly and community function are likely to improve our capacity to constrain the contribution of N-SOM to plant growth.

ACKNOWLEDGEMENTS

We thank J. Matthews, N. Ahmad, E. Herrick, B. VanDusen and the Dublin Store for valuable laboratory and field support. We thank J. Allgeier and L. Cline for their thoughtful comments on a draft of this manuscript. This work is supported by NSF award 1754369 to DRZ, and an Integrated Training in Microbial Systems (ITiMS) Fellowship to PTP.

DATA AVAILABILITY

All data will be deposited upon acceptance in Dryad. Molecular sequencing data will be uploaded to GenBank upon acceptance. Isotopic data used in this study is available onDryad at https://doi.org/10.5061/dryad.4f4qrfjbt.

REFERENCES

Averill C, Bhatnagar JM, Dietze MC, Pearse WD, Kivlin SN. 2019. Global imprint of mycorrhizal fungi on whole-plant nutrient economics. Proc Natl Acad Sci USA 116:23163–23168.

Avis PG. 2012. Ectomycorrhizal iconoclasts: the ITS rDNA diversity and nitrophilic tendencies of fetid Russula. Mycologia 104:998–1007.

Bödeker ITM, Clemmensen KE, de Boer W, Martin F, Olson Å, Lindahl BD. 2014. Ectomycorrhizal Cortinarius species participate in enzymatic oxidation of humus in northern forest ecosystems. New Phytol 203:245–256.

Bödeker ITM, Nygren CMR, Taylor AFS, Olson Å, Lindahl BD. 2009. ClassII peroxidase-encoding genes are present in a phylogenetically wide range of ectomycorrhizal fungi. ISME J 3:1387–1395.

Brooks PD, Stark JM, McInteer BB, Preston T. 1989. Diffusion method to prepare soil extracts for automated nitrogen-15 analysis. Soil Sci Soc Am J 53:1707–1711.

Cabrera ML, Beare MH. 1993. Alkaline Persulfate oxidation for determining total nitrogen in microbial biomass extracts. Soil Sci Soc Am J 57:1007–1012.

Christian N, Bever JD. 2018. Carbon allocation and competition maintain variation in plant root mutualisms. Ecol Evol 8:5792–5800.

Corrales A, Mangan SA, Turner BL, Dalling JW. 2016. An ectomycorrhizal nitrogen economy facilitates monodominance in a neotropical forest. Ecol Lett 19:383–392.

Courty P-E, François M, Marc-André S, Myriam D, Stéven Criquet, Fabio Z, Marc B, Claude P, Adrien T, Jean G, Franck R. 2016. Into the functional ecology of ectomycorrhizal communities: environmental filtering of enzymatic activities. J Ecol 104:1585–1598.

Craine JM, Elmore AJ, Aidar MPM, Bustamante M, Dawson TE, Hobbie EA, Kahmen A, Mack MC, McLauchlan KK, Michel-

sen A, Nardoto GB, Pardo LH, Peñuelas J, Reich PB, Schuur EAG, Stock WD, Templer PH, Virginia RA, Welker JM, Wright IJ. 2009. Global patterns of foliar nitrogen isotopes and their relationships with climate, mycorrhizal fungi, foliar nutrient concentrations, and nitrogen availability. New Phytol 183:980–992.

Darrouzet-Nardi A, Ladd MP, Weintraub MN. 2013. Fluorescent microplate analysis of amino acids and other primary amines in soils. Soil Biol Biochem 57:78–82.

Defrenne CE, Philpott TJ, Guichon SHA, Roach WJ, Pickles BJ, Simard SW. 2019. Shifts in ectomycorrhizal fungal communities and exploration types relate to the environment and fine-root traits across interior douglas-fir forests of Western Canada. Front Plant Sci 10:643.

Edwards IP, Zak DR. 2010. Phylogenetic similarity and structure of Agaricomycotina communities across a forested landscape. Mol Ecol 19:1469–1482.

Gardes M, Bruns TD. 1996. Community structure of ectomycorrhizal fungi in a Pinus muricata forest: above- and below-ground views. Canadian Journal of Botany 74:1572–1583.

Genre A, Lanfranco L, Perotto S, Bonfante P. 2020. Unique and common traits in mycorrhizal symbioses. Nat Rev Microbiol 18:649–660.

Hobbie EA, Agerer R. 2010. Nitrogen isotopes in ectomycorrhizal sporocarps correspond to belowground exploration types. Plant Soil 327:71–83.

Hobbie EA, Colpaert JV. 2003. Nitrogen availability and colonization by mycorrhizal fungi correlate with nitrogen isotope patterns in plants. New Phytol 157:115–126.

Hobbie EA, Hobbie JE. 2008. Natural Abundance of 15N in nitrogen-limited forests and tundra can estimate nitrogen cycling through mycorrhizal fungi: a review. Ecosystems 11:815–830.

Hobbie EA, Högberg P. 2012. Nitrogen isotopes link mycorrhizal fungi and plants to nitrogen dynamics. New Phytol 196:367–382.

Hobbie EA, Macko SA, Williams M. 2000. Correlations between foliar δ15N and nitrogen concentrations may indicate plant-mycorrhizal interactions. Oecologia 122:273–283.

Hobbie JE, Hobbie EA. 2006. ^{15}N in symbiotic fungi and plants estimates nitrogen and carbon flux rates in arctic tundra. Ecology 87:816–822.

Hogberg P, Hogberg MN, Quist ME, Ekblad A, Nasholm T. 1999. Nitrogen isotope fractionation during nitrogen uptake by ectomycorrhizal and non-mycorrhizal Pinus sylvestris. New Phytol 142:569–576.

Inselsbacher E, Näsholm T. 2012. The below-ground perspective of forest plants: soil provides mainly organic nitrogen for plants and mycorrhizal fungi. New Phytol 195:329–334.

Jones DL, Healey JR, Willett VB, Farrar JF, Hodge A. 2005. Dissolved organic nitrogen uptake by plants—an important N uptake pathway? Soil Biol Biochem 37:413–423.

Kielland K. 1994. Amino acid absorption by arctic plants: implications for plant nutrition and nitrogen cycling. Ecology 75:2373–2383.

Kohler A, Kuo A, Nagy LG, Morin E, Barry KW, Buscot F, Canbäck B, Choi C, Cichocki N, Clum A, Colpaert J, Copeland A, Costa MD, Doré J, Floudas D, Gay G, Girlanda M, Henrissat B, Herrmann S, Hess J, Högberg N, Johansson T, Khouja H-R, LaButti K, Lahrmann U, Levasseur A, Lindquist EA, Lipzen A, Marmeisse R, Martino E, Murat C, Ngan CY, Nehls U, Plett JM, Pringle A, Ohm RA, Perotto S, Peter M, Riley R, Rineau F, Ruytinx J, Salamov A, Shah F, Sun H, Tarkka M, Tritt A, Veneault-Fourrey C, Zuccaro A, Tunlid A, Grigoriev IV, Hibbett DS, Martin F. 2015. Convergent losses of decay mechanisms and rapid turnover of symbiosis genes in mycorrhizal mutualists. Nat Genet 47:410–415.

Kohzu A, Tateishi T, Yamada A, Koba K, Wada E. 2000. Nitrogen isotope fractionation during nitrogen transport from ectomycorrhizal fungi, Suillus granulatus, to the host plant, Pinus densiflora. Soil Sci Plant Nutr 46:733–739.

Koide RT, Fernandez C, Malcolm G. 2014. Determining place and process: functional traits of ectomycorrhizal fungi that affect both community structure and ecosystem function. New Phytol 201:433–439.

Kranabetter JM, Hawkins BJ, Jones MD, Robbins S, Dyer T, Li T. 2015. Species turnover (β-diversity) in ectomycorrhizal fungi linked to uptake capacity. Mol Ecol 24:5992–6005.

Kranabetter JM, MacKenzie WH. 2010. Contrasts among Mycorrhizal plant guilds in foliar nitrogen concentration and δ15N along productivity gradients of a boreal forest. Ecosystems 13:108–117.

Lilleskov EA, Fahey TJ, Horton TR, Lovett GM. 2002. Belowground ectomycorrhizal fungal community change over a nitrogen deposition gradient in Alaska. Ecology 83:104–115.

Lindahl BD, Tunlid A. 2015. Ectomycorrhizal fungi—potential organic matter decomposers, yet not saprotrophs. New Phytol 205:1443–1447.

van der Linde S, Suz LM, Orme CDL, Cox F, Andreae H, Asi E, Atkinson B, Benham S, Carroll C, Cools N, De Vos B, Dietrich H-P, Eichhorn J, Gehrmann J, Grebenc T, Gweon HS, Hansen K, Jacob F, Kristöfel F, Lech P, Manninger M, Martin J, Meesenburg H, Merilä P, Nicolas M, Pavlenda P, Rautio P, Schaub M, Schröck H-W, Seidling W, Šrámek V, Thimonier A, Thomsen IM, Titeux H, Vanguelova E, Verstraeten A, Vesterdal L, Waldner P, Wijk S, Zhang Y, Žlindra D, Bidartondo MI. 2018. Environment and host as large-scale controls of ectomycorrhizal fungi. Nature 558:243–248.

Mayor J, Bahram M, Henkel T, Buegger F, Pritsch K, Tedersoo L. 2015. Ectomycorrhizal impacts on plant nitrogen nutrition: emerging isotopic patterns, latitudinal variation and hidden mechanisms. Ecol Lett 18:96–107.

Mayor JR, Schuur EAG, Henkel TW. 2009. Elucidating the nutritional dynamics of fungi using stable isotopes. Ecol Lett 12:171–183.

McClaugherty CA, Pastor J, Aber JD, Melillo JM. 1985. Forest litter decomposition in relation to soil nitrogen dynamics and litter quality. Ecology 66:266–275.

Melillo JM, Aber JD, Linkins AE. 1989. Carbon and nitrogen dynamics along the decay continuum: plant litter to soil organic matter. Plant Soil 115:189–198.

Michelsen A, Quarmby C, Sleep D, Jonasson S. 1998. Vascular plant 15 N natural abundance in heath and forest tundra ecosystems is closely correlated with presence and type of mycorrhizal fungi in roots. Oecologia 115:406–418.

Michelsen A, Schmidt IK, Jonasson S, Quarmby C, Sleep D. 1996. Leaf 15N abundance of subarctic plants provides field evidence that ericoid, ectomycorrhizal and non-and arbuscular mycorrhizal species access different sources of soil nitrogen. Oecologia 105:53–63.

Miyauchi S, Kiss E, Kuo A, Drula E, Kohler A, Sánchez-García M, Morin E, Andreopoulos B, Barry KW, Bonito G, Buée M, Carver A, Chen C, Cichocki N, Clum A, Culley D, Crous PW, Fauchery L, Girlanda M, Hayes RD, Kéri Z, LaButti K, Lipzen A, Lombard V, Magnuson J, Maillard F, Murat C, Nolan M,

Ohm RA, Pangilinan J, de Pereira MF, Perotto S, Peter M, Pfister S, Riley R, Sitrit Y, Stielow JB, Szöllősi G, Žifčáková L, Štursová M, Spatafora JW, Tedersoo L, Vaario L-M, Yamada A, Yan M, Wang P, Xu J, Bruns T, Baldrian P, Vilgalys R, Dunand C, Henrissat B, Grigoriev IV, Hibbett D, Nagy LG, Martin FM. 2020. Large-scale genome sequencing of mycorrhizal fungi provides insights into the early evolution of symbiotic traits. Nat Commun 11:5125.

Moeller HV, Peay KG, Fukami T. 2014. Ectomycorrhizal fungal traits reflect environmental conditions along a coastal California edaphic gradient. FEMS Microbiol Ecol 87:797–806.

Näsholm T, Kielland K, Ganeteg U. 2009. Uptake of organic nitrogen by plants. New Phytol 182:31–48.

Nilsson LO, Giesler R, Bååth E, Wallander H. 2005. Growth and biomass of mycorrhizal mycelia in coniferous forests along short natural nutrient gradients. New Phytol 165:613–622.

Nilsson RH, Larsson K-H, Taylor AFS, Bengtsson-Palme J, Jeppesen TS, Schigel D, Kennedy P, Picard K, Glöckner FO, Tedersoo L, Saar I, Kõljalg U, Abarenkov K. 2019. The UNITE database for molecular identification of fungi: handling dark taxa and parallel taxonomic classifications. Nucl Acids Res 47:D259–D264.

Nordin A, Schmidt IK, Shaver GR. 2004. Nitrogen uptake by arctic soil microbes and plants in relation to soil nitrogen supply. Ecology 85:955–962.

Orwin KH, Kirschbaum MUF, John MGS, Dickie IA. 2011. Organic nutrient uptake by mycorrhizal fungi enhances ecosystem carbon storage: a model-based assessment. Ecol Lett 14:493–502.

Pardo LH, Templer PH, Goodale CL, Duke S, Groffman PM, Adams MB, Boeckx P, Boggs J, Campbell J, Colman B, Compton J, Emmett B, Gundersen P, Kjønaas J, Lovett G, Mack M, Magill A, Mbila M, Mitchell MJ, McGee G, McNulty S, Nadelhoffer K, Ollinger S, Ross D, Rueth H, Rustad L, Schaberg P, Schiff S, Schleppi P, Spoelstra J, Wessel W. 2006. Regional assessment of n saturation using foliar and root δ^{15}N. Biogeochemistry 80:143–171.

Pastor J, Aber JD, McClaugherty CA, Melillo JM. 1984. Aboveground production and N and P cycling along a nitrogen mineralization gradient on Blackhawk Island, Wisconsin. Ecology 65:256–268.

Peay KG, Russo SE, McGuire KL, Lim Z, Chan JP, Tan S, Davies SJ. 2015. Lack of host specificity leads to independent assortment of dipterocarps and ectomycorrhizal fungi across a soil fertility gradient. Ecol Lett 18:807–816.

Pellitier PT, Zak DR. 2018. Ectomycorrhizal fungi and the enzymatic liberation of nitrogen from soil organic matter: why evolutionary history matters. New Phytologist 217:68–73.

Phillips RP, Brzostek E, Midgley MG. 2013. The mycorrhizal-associated nutrient economy: a new framework for predicting carbon–nutrient couplings in temperate forests. New Phytol 199:41–51.

Read D. 1991. Mycorrhizas in ecosystems. Experientia 47:376–391.

Read DJ, Perez-Moreno J. 2003. Mycorrhizas and nutrient cycling in ecosystems: a journey towards relevance? New Phytol 157:475–492.

Robinson D. 2001. δ15N as an integrator of the nitrogen cycle. Trends Ecol Evol 16:153–162.

Rothstein DE. 2009. Soil amino-acid availability across a temperate-forest fertility gradient. Biogeochemistry 92:201–215.

Smith ME, Henkel TW, Aime MC, Fremier AK, Vilgalys R. 2011. Ectomycorrhizal fungal diversity and community structure on three co-occurring leguminous canopy tree species in a Neotropical rainforest. New Phytol 192:699–712.

Smith SE, Read DJ. 2010. Mycorrhizal symbiosis. Cambridge: Academic Press.

Sterkenburg E, Clemmensen KE, Ekblad A, Finlay RD, Lindahl BD. 2018. Contrasting effects of ectomycorrhizal fungi on early and late stage decomposition in a boreal forest. ISME J 12:2187–2197.

Suz LM, Barsoum N, Benham S, Dietrich H-P, Fetzer KD, Fischer R, García P, Gehrman J, Kristöfel F, Manninger M, Neagu S, Nicolas M, Oldenburger J, Raspe S, Sánchez G, Schröck HW, Schubert A, Verheyen K, Verstraeten A, Bidartondo MI. 2014. Environmental drivers of ectomycorrhizal communities in Europe's temperate oak forests. Mol Ecol 23:5628–5644.

Taylor AFS, Fransson PM, Högberg P, Högberg MN, Plamboeck AH. 2003. Species level patterns in 13C and 15N abundance of ectomycorrhizal and saprotrophic fungal sporocarps. New Phytol 159:757–774.

Taylor AFS, Högbom L, Högberg M, Lyon AJE, Näsholm T, Högberg P. 1997. Natural 15N abundance in fruit bodies of ectomycorrhizal fungi from boreal forests. New Phytol 136:713–720.

Taylor AFS, Martin F, Read DJ. 2000. Fungal diversity in ectomycorrhizal communities of Norway spruce [*Picea abies* (L.) Karst] and Beech (*Fagus sylvatica* L.) along north-south transects in Europe. In: Schulze E-D, Ed. Carbon and nitrogen cycling in European forest ecosystems. Ecological studies, . Berlin: Springer. pp 343–365.

Tedersoo L, Naadel T, Bahram M, Pritsch K, Buegger F, Leal M, Kõljalg U, Põldmaa K. 2012. Enzymatic activities and stable isotope patterns of ectomycorrhizal fungi in relation to phylogeny and exploration types in an afrotropical rain forest. New Phytol 195:832–843.

Tedersoo L, Smith ME. 2013. Lineages of ectomycorrhizal fungi revisited: foraging strategies and novel lineages revealed by sequences from belowground. Fungal Biol Rev 27:83–99.

Terrer C, Jackson RB, Prentice IC, Keenan TF, Kaiser C, Vicca S, Fisher JB, Reich PB, Stocker BD, Hungate BA, Peñuelas J, McCallum I, Soudzilovskaia NA, Cernusak LA, Talhelm AF, Van Sundert K, Piao S, Newton PCD, Hovenden MJ, Blumenthal DM, Liu YY, Müller C, Winter K, Field CB, Viechtbauer W, Van Lissa CJ, Hoosbeek MR, Watanabe M, Koike T, Leshyk VO, Polley HW, Franklin O. 2019. Nitrogen and phosphorus constrain the CO_2 fertilization of global plant biomass. Nat Climate Change 9:684–689.

Terrer C, Vicca S, Hungate BA, Phillips RP, Prentice IC. 2016. Mycorrhizal association as a primary control of the CO_2 fertilization effect. Science 353:72–74.

Vitousek P. 1982. Nutrient cycling and nutrient use efficiency. Am Nat 119:553–572.

Wang Y, Naumann U, Wright ST, Warton DI. 2012. mvabund–an R package for model-based analysis of multivariate abundance data. Methods Ecol Evol 3:471–474.

Werner RA, Schmidt H-L. 2002. The in vivo nitrogen isotope discrimination among organic plant compounds. Phytochemistry 61:465–484.

Wieder WR, Cleveland CC, Smith WK, Todd-Brown K. 2015. Future productivity and carbon storage limited by terrestrial nutrient availability. Nat Geosci 8:441–444.

Wolfe BE, Tulloss RE, Pringle A. 2012. The irreversible loss of a decomposition pathway marks the single origin of an ectomycorrhizal symbiosis. PLoS ONE 7:e39597.

Yano Y, Shaver GR, Giblin AE, Rastetter EB. 2010. Depleted 15N in hydrolysable-N of arctic soils and its implication for mycorrhizal fungi–plant interaction. Biogeochemistry 97:183–194.

Zak D, Grigal D. 1991. Nitrogen mineralization, nitrification and denitrification in upland and wetland ecosystems. Oecologia 88:189–196.

Zak DR, Groffman PM, Pregitzer KS, Christensen S, Tiedje JM. 1990. The vernal dam: plant-microbe competition for nitrogen in northern hardwood forests. Ecology 71:651–656.

Zak DR, Pellitier PT, Argiroff W, Castillo B, James TY, Nave LE, Averill C, Beidler KV, Bhatnagar J, Blesh J, Classen AT, Craig M, Fernandez CW, Gundersen P, Johansen R, Koide RT, Lilleskov EA, Lindahl BD, Nadelhoffer KJ, Phillips RP, Tunlid A. 2019. Exploring the role of ectomycorrhizal fungi in soil carbon dynamics. New Phytol 223:33–39.

Zak DR, Pregitzer KS. 1990. Spatial and temporal variability of nitrogen cycling in northern lower Michigan. For Sci 36:367–380.

Zak DR, Pregitzer KS, Host GE. 1986. Landscape variation in nitrogen mineralization and nitrification. Can J For Res 16:1258–1263.